Journal of Materials Chemistry B

PAPER

View Article Online
View Journal | View Issue

Cite this: J. Mater. Chem. B, 2014, 2, 3282

Revisiting the complexation between DNA and polyethylenimine – when and where –S–S– linked PEI is cleaved inside the cell†

Yongzheng Ma*[a] and Chi Wu[ab]

Received 6th January 2014
Accepted 1st March 2014

DOI: 10.1039/c4tb00031e

www.rsc.org/MaterialsB

As a non-viral gene vector, long PEI chains are more effective but also more cytotoxic. To solve this problem, people have tried to use disulfide (–S–S–) to link short PEI chains into a long one to generate highly efficient and less cytotoxic gene vectors because –S–S– is degradable inside the cell. In order to investigate when and where –S–S– is cleaved during intracellular trafficking, we designed and synthesized rhodamine B labeled linear PEI chains ($M_n \approx 3$ kg mol^{-1}) with one end modified with a mercapto-group so that they can be coupled together *via* one disulfide bond in the middle and one rhodamine B molecule on each side of the disulfide bond, where fluorescence is self-quenched because two rhodamine B molecules are closely linked together. The cleavage of the –S–S– bond separates the two rhodamine B molecules and enhances their fluorescent intensity. In addition, plasmid DNA was also modified with bodipy, a FRET donor of rhodamine B. Using this specially prepared PEI, we studied the intracellular trafficking of the PEI/DNA polyplexes by using flow cytometry and confocal laser scanning microscopy. Our results reveal that (1) DNA is gradually dissociated from the polyplex before the disulfide bond's cleavage; (2) some of polyplexes escaped from endosomes before reaching lysosomes; and (3) the disulfide bonds are mainly cleaved inside lysosomes at ~5 h post-transfection.

1. Introduction

Gene therapy has been proposed to cure various diseases.[1,2] To achieve a therapeutic effect, an effective gene vector is needed.[3] Due to their large packing size, low immunogenicity, and high design flexibility, different non-viral gene vectors,[4–6] especially cationic polymers, have been developed. In the past three decades, hundreds, if not thousands, of synthetic cationic polymers have been prepared and studied. Among them, polyethylenimine (PEI) remains as one of the most efficient non-viral gene vectors since it was introduced by Behr in 1995.[7,8]

Many efforts have been devoted to studying the origins of PEI's high transfection efficiency.[9–13] However, PEI chains have different topologies (linear and branched) for a given molar mass and different molar masses for a given chain morphology, making studies complicated and less defined, especially when *in vitro* cellular and *in vivo* animal tests are involved. To deliver a therapeutic gene into a specific kind of cells, the gene and its vector have to overcome many obstacles.[14,15] Some previous studies have shown that following endocytosis, the PEI/DNA complexes (polyplexes) escaped during the endocytic pathway *via* the "proton sponge effect".[16,17] Namely, partially protonated PEI chains absorb more protons inside the endocytic vesicles embedded with ATPase proton pumps, accompanied by an influx of chloride counter ions, so that the higher osmotic pressure accumulated inside would ultimately rupture the endocytic vesicles. However, such an assumption could not explain why longer PEI chains are better than shorter ones at promoting gene transfection, because short chains, in principle, would lead to higher osmotic pressure.

Godbey *et al.*[18] tried to track the intracellular pathway of fluorescence-labeled polyplexes made of branched PEI inside EA.hy 926 cells. Their results revealed that both free PEI chains and PEI/DNA polyplexes could be found inside the nuclei. Up to now, it is still unclear whether large polyplexes could be translocated from the cytosol into the nucleus, but their results did show that PEI/DNA polyplexes can effectively escape during the endocytic pathway. In addition, the condensation ability of PEI might also play a key role.[19]

Recently, we did a systematic study of the complexation between DNA and PEI with different chain topologies and lengths, for the first time, by using a combination of static and dynamic laser light scattering.[20] We revealed that when the N/P ratio is higher than 6, most of the polyplexes contain only one DNA chain and the initial PEI chain topology affects the final

[a]Department of Chemistry, The Chinese University of Hong Kong, Shatin, N. T., Hong Kong. E-mail: ericyongzheng@126.com

[b]The Hefei National Laboratory of Physical Science at Microscale, Department of Chemical Physics, University of Science and Technology of China, Hefei, Anhui, 230026, China

† Electronic supplementary information (ESI) available: Synthesis details for the probe, the absorption and emission spectra of B-DNA and Rho-PEI, the emission intensity of polyplexes and NMR spectra of the probe. See DOI: 10.1039/c4tb00031e

morphology of the polyplexes. Linear PEI chains lead to an "onion-like" morphology so that abundant anionic proteins inside the cytosol can peal the cationic PEI chains on/in each polyplexes in a layer-by-layer fashion to release the DNA chain inside. Therefore, polyplexes made of linear PEI chains are less stable than those made of branched PEI chains that act as a "cross-linking" agent inside, so that releasing DNA from branched PEI/DNA polyplexes is relatively more difficult.

Our results are also proved by the study of fluorescence resonance energy transfer (FRET). Itaka *et al.*[19] monitored the intracellular trafficking of PEI/DNA polyplexes and found that DNA condensed with linear PEI chains can be quickly delivered into the cytoplasm and easily released. Furthermore, we found that apart from the condensation and dissociation of DNA, uncomplexed PEI chains with a size larger than ~15 nm which are free in the solution mixture of DNA and PEI also play a critical role in promoting gene transfection,[21,22] leading to speculation that it is those free chains that interact with signal proteins to block inter-vesicular fusion so that the ingested PEI/DNA polyplexes have less chance of being delivered/developed into lysosomes and a higher probability of escape from endosomes.

Previously, in order to reduce the cytotoxicity of long PEI chains, disulfide-connected PEI chains were used because the cytosol is a redox environment.[23] Many degradable PEI chains have been designed, prepared and tested for gene delivery.[24–27] However, most of these studies were focused on polymer preparation. The exact roles that the disulfide bonds play inside the polyplexes are less studied. Lee *et al.*[28] confirmed the disulfide bonds can be cleaved during intracellular trafficking. Yang *et al.*[29] evaluated disulfide reduction during receptor-mediated endocytosis by using FRET imaging and found that the reduction of the disulfide bonds occurred along the entire folate-receptor endocytic pathway. However, the probes they used were receptor-dependent small molecules, which might lead to a reduction mechanism different from that of degradable PEI chains inside the polyplexes. In addition, Austin *et al.*[30] reported that recycling endosomes, late-endosomes, and lysosomes were not actually reducing but oxidizing, comparable with the conditions in the endoplasmic reticulum. It is those controversial and incomplete results that prompted us to design the current study to find when and where the –S–S– bonds of the PEI chains inside the polyplexes are cleaved and the exact roles of the –S–S– bonds apart from reducing the PEI's cytotoxicity.

To address these questions, we designed and synthesized a rhodamine B labeled linear PEI as a probe by coupling two short linear PEI chains together with fluorescent molecules and a disulfide linker. In order to eliminate the chain length effect, we purposely prepared linear PEI with $M_n \approx 3000$ g mol^{-1} as the initial short chain, which is already long enough to interfere with the signal proteins involved in inter-vesicular fusion. In our design, the fluorescence of two rhodamine B molecules is self-quenched because they are linked by a short disulfide bond.[31–33] The cleavage of –S–S– separates the two rhodamine B molecules and enhances the fluorescent intensity. In addition, the plasmid DNA was modified with bodipy, a FRET donor of rhodamine B. The FRET occurs once DNA is condensed by the rhodamine B-modified PEI chains, which enable us to monitor the trafficking of the polyplexes and probe when and where the disulfide bonds are cleaved inside the cell.

2. Experimental

2.1 Materials and cell lines

Linear and branched polyethylenimines (lPEI-25k and bPEI25k, $M_w = 25$ kg mol^{-1}) were purchased from Polysciences and Sigma-Aldrich, respectively, and used without further purification. Methyl *p*-toluenesulfonate from Sigma-Aldrich was distilled and stored under nitrogen. 2-Ethyl-2-oxazoline was purchased from Sigma-Aldrich and purified by vacuum distillation over CaH_2. Acetonitrile from RCI Labscan was dried over CaH_2 and distilled under dry nitrogen.

N,*N*-Diisopropylethylamine (DIEA), ethane-1,2-dithiol (EDT), triisopropylsilane (TIS), piperidine, rhodamine B and Sephadex G-50 were purchased from Sigma-Aldrich. 1-Ethyl-3-(3-dimethyl aminopropyl) carbodiimide hydrochloride (EDC), *N*-hydroxybenzotriazole (HOBt), *N*-Fmoc-*S*-tritylcysteine (Fmoc-Cys(trt)-OH), and glycine *tert*-butyl ester hydrochloride (H-Gly-otBu) were obtained from GL Biochem Ltd (Shanghai, China). *N*,*N*-Dimethylformamide (DMF) from RCI Labscan was dried over CaH_2 and purified by vacuum distillation. All other chemicals and solvents were used as received without further purification.

Initial plasmid DNA (pGL3) with a SV40 promoter and an enhancer sequence encoding firefly luciferase was purchased from Promega (Madison, USA). A large amount of this plasmid DNA was made with a Qiagen Plasmid Maxi Kit (Qiagen, Germany). Fetal bovine serum (FBS), penicillin–streptomycin and Dulbecco's modified Eagle's medium (DMEM) were products of GIBCO (NY, USA). 3-(4,5-Dimethylthiazol-2-yl)-2,5-diphenyltetrazolium bromide (MTT) was purchased from Sigma-Aldrich. A Label IT Amine Nucleic Acid Modifying Kit from Mirus was used to modify the plasmid DNA with amino-groups. Lysosensor™ Green, Celllight early endosomes-GFP and bodipy FL NHS ester were purchased from Invitrogen. Dextran sulfate (DS, $M_w = 10$ kg mol^{-1}) and tris(2-carboxyethyl)phosphine hydrochloride (TCEP) were products of Sigma-Aldrich. HepG2 cells were grown at 37 °C, in 5% CO_2 in DMEM supplemented with 10% FBS, penicillin at 100 units per mL and streptomycin at 100 μg mL^{-1}.

2.2 Synthesis of linear polyethylenimine (lPEI), Rho-Cys-Gly-PEI (Rho-PEI) and (Rho-Cys-Gly-PEI)$_2$ ((Rho-PEI)$_2$)

Complete synthesis details for linear polyethylenimine (lPEI), Rho-Cys-Gly-PEI (Rho-PEI) and (Rho-Cys-Gly-PEI)$_2$ ((Rho-PEI)$_2$) may be found in the ESI.† Scheme 1 summarizes our synthesis procedure.

2.3 Characterization

A Bruker Advanced III 400 NMR spectrometer was used. The chemical shifts (δ) were reported in ppm with the solvent resonance as the internal standard relative to $CDCl_3$ (δ 7.26), CD_3OD (δ 3.31) or D_2O (δ 4.79) for ^{1}H. All the ^{1}H NMR

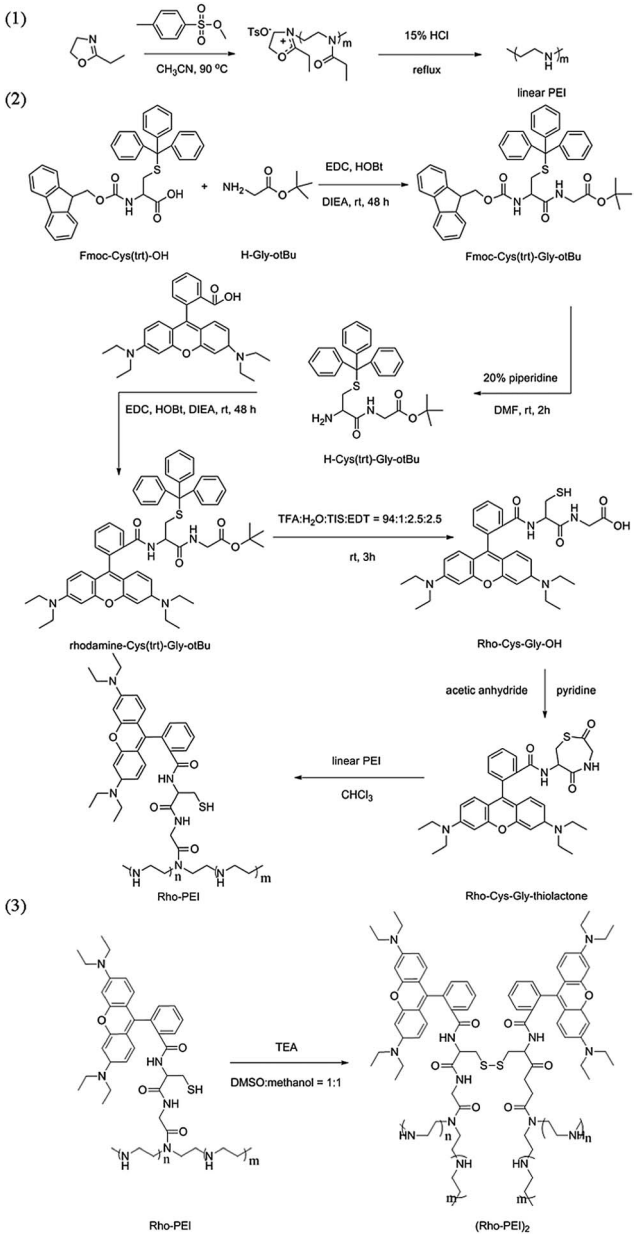

Scheme 1 Schematic of the synthesis of probes (1) linear PEI; (2) Rho-PEI; and (3) $(Rho\text{-}PEI)_2$.

measurements were carried out at room temperature. Mass spectra (ESI-MS) were obtained with a HP 5989B spectrometer and determined at an ionizing voltage of 70 eV; the relevant data are given as m/z.

2.4 Size exclusion chromatography (SEC)

The relative number- and weight-averaged molar masses (M_n and M_w) were determined at 35 °C by SEC (Waters 1515) with three Waters Styragel columns (HR2, HR4, HR6), and two detectors: refractive index (RI, Wyatt WREX-02) and multi-angle laser light scattering (MALLS, Wyatt DAWN EOS). THF was used as the eluent at a flow rate of 1.0 mL min^{-1} and the conventional universal calibration with linear polystyrene standards was used. The MALLS detector used a GaAs laser (685 nm and 30 mW) and had 18 diodes placed at different angles, ranging from 22.5 to 147.0°. The data were analyzed using the ASTRA for Windows software (Ver. 4.90.07, Wyatt). For both SEC-RI and SEC-MALLS measurements, 1 mL of polymer solution (2–8 mg mL^{-1}, depending on the molar mass) was pre-filtered through a 0.2 μm PVDF filter before injection.

2.5 Laser light scattering (LLS)

A commercial LLS instrument (ALV5000) with a vertically polarized 22 mV He–Ne laser (632.8 nm, Uniphase) was used to detect the molecular weight of $(Rho\text{-}PEI)_2$. In static LLS, we can obtain the weight-averaged molar mass (M_w) and the z-averaged root-mean square radius of gyration ($\langle R_g\rangle_z$) of scattering objects in a sufficiently dilute solution/dispersion from the angular and concentration dependence of the excess absolute scattering intensity (Rayleigh ratio, $R_{vv}(q)$) as $KC/R_{vv}(q) \approx (1 + q^2R_g^2/3)/M_w$ where $K = 4\pi^2(dn/dc)^2/(N_A\lambda_o^4)$ and $q = (4\pi n/\lambda_o)\sin(\theta/2)$, with dn/dC, N_A, λ_o, n and θ being the specific refractive index increment, the Avogadro constant number, the incident wavelength in vacuum, the refractive index of solvent, and the scattering angle, respectively. Note that we have neglected the concentration correction here. To measure the weight averaged molar mass of $(Rho\text{-}PEI)_2$, both Rho-PEI and $(Rho\text{-}PEI)_2$ solutions were prepared in a 30 mM NaCl solution and then clarified by a 0.45 μm filter. The solutions were measured by dynamic LLS at a low scattering angle of 20°. The weight averaged molar mass (M_w) of $(Rho\text{-}PEI)_2$ was calculated from $M_{Rho\text{-}PEI} \times (\langle I_0\rangle_{(Rho\text{-}PEI)_2}/C_{(Rho\text{-}PEI)_2})/(\langle I_0\rangle_{Rho\text{-}PEI}/C_{Rho\text{-}PEI})$, where $C_{Rho\text{-}PEI}$, $C_{(Rho\text{-}PEI)_2}$, $\langle I_0\rangle_{Rho\text{-}PEI}$ and $\langle I_0\rangle_{(Rho\text{-}PEI)_2}$ are the concentrations and the time averaged scattering intensities of Rho-PEI and $(Rho\text{-}PEI)_2$ at the zero scattering angle, respectively.

In dynamic LLS, the Laplace inversion of each measured time correlation function ($G^{(2)}(q, t)$) can be related to a line-width distribution $G(\Gamma)$. For a diffusion relaxation, Γ is further related to the translational diffusion coefficient D by $(\Gamma/q^2)_{c\to 0, q\to 0} = D$. Therefore, $G(\Gamma)$ can be converted into a translational diffusion coefficient distribution $G(D)$ or a hydrodynamic radius distribution $f(Rh)$ using the Stokes–Einstein equation, $R_h = k_BT/(6\pi\eta D)$, where k_B, T, and η are the Boltzmann constant, the absolute temperature, and the solvent viscosity, respectively.

2.6 Fluorescent labeling of plasmid DNA

Plasmid DNA was modified with amino-groups using a Label IT Amine Nucleic Acid Modifying Kit at a 0.2 : 1 (mass label reagent/mass nucleic acid) ratio according to the manufacturer's instructions. Amine modified DNA was diluted in 200 mM MOPS and stored at −20 °C. 80 μg of purified amine-modified DNA was reacted with 90 μg bodipy FL NHS ester in DMSO (5 μL) and 100 mM $NaHCO_3$ (20 μL, pH = 8.5, freshly prepared) for 12 hours at room temperature in the dark. To purify the labeled DNA, the solution was precipitated in ethanol, and washed extensively with 70% ethanol. The final product bodipy-DNA (B-DNA) was dissolved in 1 × Tris–EDTA buffer and stored at −20 °C.

2.7 Cytotoxicity of PEI vectors

The MTT assay was used to test the cytotoxicity of each polymer used. PEI solutions with different concentrations were prepared in DMEM. HepG2 cells were seeded in 96-well culture plates at 10^4 cells per well in 100 μL DMEM medium containing 10% FBS and antibiotics. 24 h later the PEI solution under study was added to each well. The treated cells were incubated in a humidified environment with 5% CO_2 at 37 °C for 48 h. The MTT reagent (in 20 μL PBS, 5 mg mL^{-1}) was added to each well and further incubated at 37 °C for 4 h. The medium was then removed and replaced with 100 μL of DMSO. The plate was gently agitated for 30 min before the absorbance (A) at 490 nm was recorded by a microplate reader (Bio-rad, USA). The cell viability was calculated as viability = $(A_{treated} - A_{blank})/(A_{control} - A_{blank}) \times 100\%$, where $A_{treated}$, A_{blank} and $A_{control}$ are the absorbance of the cells treated with PEI, fresh culture medium and without any treatment, respectively. Each experiment condition was done in triplicate. The data is shown as the mean value plus standard deviation (±SD).

2.8 Gel retardation assay of DNA complexation

The PEI/DNA polyplexes with different desired N/P ratios (the ratio of nitrogen atoms on PEI to phosphates on plasmid DNA) were prepared by adding an appropriate amount of PEI (5 μL) to 0.4 μg DNA (5 μL) in PBS. The resultant dispersions of polyplexes were incubated at room temperature for 5 min and loaded on a 0.8% (w/v) agarose gel containing ethidium bromide in TAE (Tris–acetate) buffer. Gel electrophoresis was carried out at 100 V. After 1 h, the DNA bands in the gel were visualized with a UV (254 nm) illuminator and photographed with a Vilber Lourmat imaging system.

2.9 *In vitro* gene transfection

The gene transfection experiments were performed in HepG2 cells using the plasmid pGL3 as an exogenous reporter gene. Gene transfection was conducted using PEI/DNA polyplexes with different N/P ratios (10 : 1, 15 : 1, 20 : 1, 25 : 1 and 30 : 1). The cells were seeded in a 48 well plate at an initial density of 3 $\times 10^4$ per well for 24 h before the gene transfection experiments were carried out. Each PEI/DNA polyplex dispersion with a given N/P ratio was diluted in complete DMEM medium (10% FBS, 100 units per mL penicillin and 100 μg mL^{-1} streptomycin) (200 μL), and then administered to the cells at a final concentration of 0.4 μg DNA per well. After 4 h, the transfection medium was removed and fresh DMEM medium (500 μL per well) was added. The cells were further cultured for 48 h before the transgene expression level was evaluated. A GloMax 96 microplate luminometer (Promega, USA) and the Bio-Rad protein assay reagent were used to determine the transfection efficiency of the PEI/DNA polyplexes, which is expressed as a relative luminescence unit (RLU) per cellular protein (mean ± SD of triplicates).

2.10 Fluorometric analysis

The absorption and emission spectra of fluorescence-labeled samples were recorded on Gary 5G UV/Vis/NIR and Hitachi F-4500 spectrofluorometers, respectively. To detect B-DNA released from the polyplexes, Rho-PEI/B-DNA, $(Rho\text{-}PEI)_2$/B-DNA and lPEI/B-DNA at N/P = 3 were prepared. The final DNA concentration was kept constant (0.04 μg μL^{-1} B-DNA in PBS). After 5 min of incubation at room temperature, 2 μL DS (0.1 g mL^{-1}) was added into 200 μL of each polyplex solution. To study the cleavage of disulfide bonds, Rho-PEI/DNA, $(Rho\text{-}PEI)_2$/DNA, Rho-PEI/B-DNA and $(Rho\text{-}PEI)_2$/B-DNA were prepared at N/P = 3. 10 μL of TCEP (0.1 M) was added into 200 μL of each polyplex solution. The fluorescence intensity of each solution was recorded by a spectrofluorometer in real time (excitation/emission: 488/512, 488/580 and 543/580).

2.11 Flow cytometry

For the flow cytometry experiments, HepG2 cells were seeded in a 12-well plate at an initial density of 1.2 $\times 10^5$ cells per well. After 24 h, fluorescence-labeled PEI/DNA polyplexes (N/P = 3) with an additional 7-fold free unlabeled lPEI chains were diluted in complete DMEM (500 μL) and then administered to the cells at a final concentration of 1.6 μg DNA per well. After 4 h, the transfection medium was removed and fresh DMEM was supplied. The cells were incubated at 37 °C and harvested after different desired incubation times. The harvested cells were briefly rinsed twice with PBS, and further detached by 0.05% trypsin–EDTA. Finally, the cells were washed twice with PBS, then resuspended in 4% paraformaldehyde and stored at 4 °C. The fluorescence intensity of cells was recorded by using a FC 500 flow cytometry system (Beckman Coulter, USA). For each sample, 10^4 gated events were collected. The fluorophore was excited at 488 nm and detected at 525BP (515 nm–535 nm) and 575BP (567.5 nm–582.5 nm). The fluorescence intensity was displayed using a logarithmic scale and analyzed with tetraCXP software (Beckman Coulter).

2.12 Confocal laser scanning microscopy

3 $\times 10^5$ HepG2 cells were cultured in a μ-Dish 35 mm (ibidi GmbH, Germany) for 24 h before the transfection experiment was carried out (optionally, 30 μL Celllight early endosomes-GFP was administered for 12 h before the transfection experiment was carried out). Fluorescence-labeled PEI/DNA polyplexes (N/P = 3) with an additional 7-fold free unlabeled lPEI chains were diluted in complete DMEM (1 mL) and then administered to the cells at a final concentration of 3.2 μg DNA per dish. After 4 h, the transfection medium was removed. (Optionally, 1 μL Lysosensor™ Green diluted in 1 mL DMEM was added to the cells to stain the lysosome for 15 min.) After that, the cells were washed twice with PBS and supplied with fresh DMEM. Live cell imaging was performed for 20 h using a Nikon C1si confocal laser scanning microscope equipped with a spectral imaging detector (Nikon, Japan) and an INU stage-top incubator (Tokai Hit, Japan). Image sequences were captured at approximately 1 h intervals. Bodipy, Celllight early endosomes-GFP and Lysosensor™ Green were visualized by 488 nm excitation and the

rhodamine B was excited at 543 nm. The corresponding emissions were detected at channels 515/30 and 605/75 nm, respectively. All the images were analyzed using the Nikon EZ-C1 software.

3. Results and discussion

The GPC result of poly(2-ethyl-2-oxaline) (PETOZ) shows that lPEI has a number-averaged molar mass of ~3.2 kg mol^{-1}. After it was labeled with rhodamine B, the integrals of rhodamine B and lPEI chemical shifts in the NMR spectra reveal that on average only one rhodamine B was conjugated to each PEI chain, as shown in Fig. 1. Therefore, the number averaged molar mass of Rho-PEI is ~3.8 kg mol^{-1}. The formation of a disulfide bond between the thiol groups on two Rho-PEI chains results in $(\text{Rho-PEI})_2$ with a number-averaged molar mass of ~7.6 kg mol^{-1}. Consequently, two rhodamine B molecules were symmetrically located at each end of a disulfide bond, with reduced emission intensity due to the fluorescence self-quenching (Fig. S1†). Fig. 2 shows that when the dimerized state $(\text{Rho-PEI})_2$ was reduced back to the monomeric Rho-PEI state *in vitro*, the emission intensity increases ~1.5 fold.

Fig. 3 shows that the cytotoxicity of both Rho-PEI and $(\text{Rho-PEI})_2$ increases with the polymer concentration, where both bPEI-25k and lPEI-25k are used as controls. Note that in a normal concentration range of 10^{-3} to 10^{-2} mg mL^{-1} used for gene transfection, both Rho-PEI and $(\text{Rho-PEI})_2$ are less cytotoxic than bPEI-25k and lPEI-25k. The cytotoxicity of long cationic chains has been attributed to the disruption of the anionic membranes of the cell and different organelles so that the cell undergoes necrosis.[8] Also note that linking two Rho-PEI chains together only slightly increases the cytotoxicity, compared with single Rho-PEI chains.

Fig. 4 shows that both Rho-PEI and $(\text{Rho-PEI})_2$ are able to effectively condense plasmid DNA when the N/P ratio reaches ~3, indicated by the disappearance of the free DNA strip. Indeed, at N/P ~ 5, the $(\text{Rho-PEI})_2$/DNA polyplexes start to migrate in the opposite direction. This indicates that using the disulfide bond to link two Rho-PEI chains together to form a longer $(\text{Rho-PEI})_2$ chain helps the formation of the PEI/DNA polyplexes. Note that in comparison with lPEI-25k and bPEI-25k, a slightly higher concentration of Rho-PEI or $(\text{Rho-PEI})_2$ is required to condense a given plasmid DNA chain, because long cationic chains are more effective in entropy-driven complexation and large rhodamine B moieties sterically hinder the electrostatic interaction between PEI and DNA.

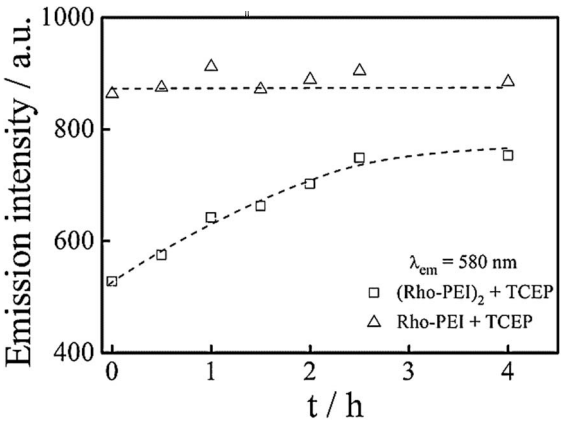

Fig. 2 Fluorescence intensities of $(\text{Rho-PEI})_2$ and Rho-PEI in PBS treated with tris(2-carboxyethyl)phosphine hydrochloride (TCEP, 0.1 M).

Fig. 5 shows that Rho-PEI and $(\text{Rho-PEI})_2$ chains are 10–100 times more efficient for transfection than longer lPEI-25k and bPEI-25k chains. Due to their high molecular weight, lPEI-25k and bPEI-25k showed higher cytotoxicity above N/P ratios of 20. Consequently, the transfection efficiencies were decreased compared to Rho-PEI and $(\text{Rho-PEI})_2$. Our previous studies showed that most of the cationic polymer chains are actually not complexed with DNA in a mixture of polymer and DNA, especially when N/P > 6.[20] We have confirmed that it is those free PEI chains with a size larger than ~15 nm that promote gene transfection.[21] This is why we purposely designed Rho-PEI with a chain length longer than ~15 nm. In addition, the hydrophobic xanthene moiety of rhodamine B in Rho-PEI and $(\text{Rho-PEI})_2$ interacts with cytoplasmic membranes, which may

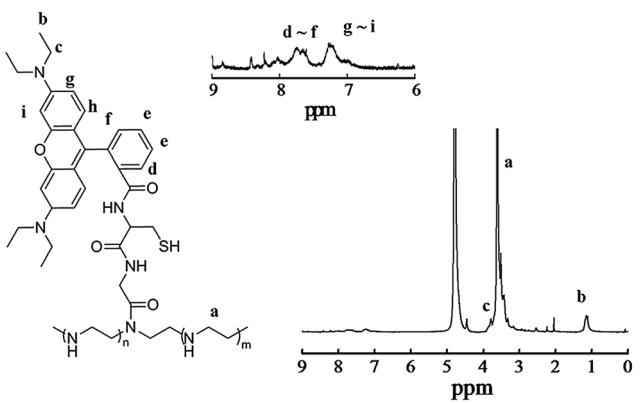

Fig. 1 ^{1}H NMR spectra of Rho-PEI in D_2O.

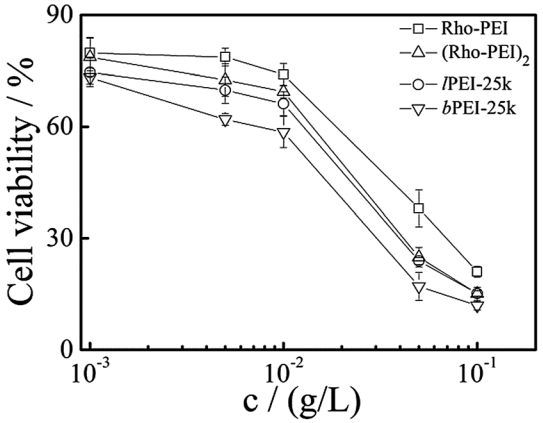

Fig. 3 Polymer concentration dependence of relative cell viability of Rho-PEI, $(\text{Rho-PEI})_2$, lPEI-25k and bPEI-25k in HepG2 cells.

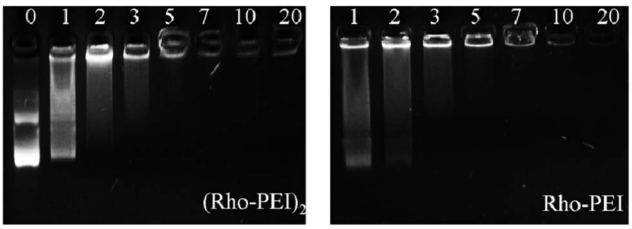

Fig. 4 N/P ratio dependence gel retardation assay of $(Rho\text{-}PEI)_2$/DNA and Rho-PEI/DNA polyplexes, where naked DNA (N/P = 0) was used as a control.

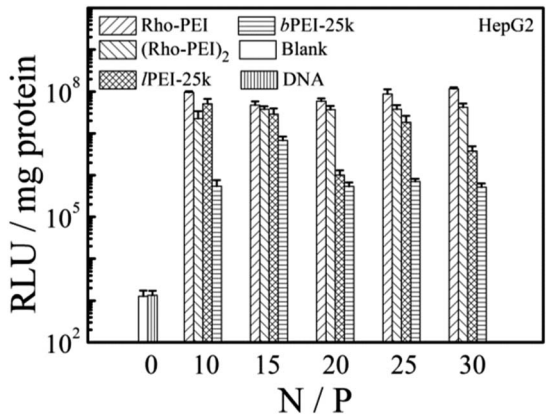

Fig. 5 N/P ratio dependence of *in vitro* gene transfection efficiency of different PEI/DNA polyplexes in HepG2 cells in the presence of serum.

increase the uptake of polyplexes. Consequently, the transfection efficiency is enhanced. Fig. 5 clearly shows that both Rho-PEI and $(Rho\text{-}PEI)_2$ are effective gene vectors, so we can use them to probe the intracellular trafficking of the polyplexes.

Since anionic plasmid DNA is labeled with bodipy (denoted as B-DNA hereafter), a FRET donor of rhodamine B (Fig. S2†), its complexation with rhodamine labeled cationic PEI results in a fluorescence intensity change (lPEI/B-DNA, Fig. S3 and S4;† Rho-PEI/B-DNA, Fig. S5;† and $(Rho\text{-}PEI)_2$/B-DNA, Fig. S6.†) All the polyplexes were prepared at N/P ratio of 3. This is because we want to avoid the interference of free rhodamine B-labeled PEI chains in the solution when the N/P is higher. Besides, lots of anionic proteins are present in the cytosol, which can replace anionic DNA chains inside the polyplexes after they enter into the cell, leading to their destabilization. To test this destabilization effect, we used anionic dextran sulfate chains to mimic proteins.

Fig. 6 shows that after the addition of dextran sulfate, the intensity ratio of the fluorescence emitted at two different wavelengths by $(Rho\text{-}PEI)_2$/B-DNA increases, but that of Rho-PEI/B-DNA remains constant in the first 2 h, and approaches a plateau value after ~4 h. This shows that as anionic B-DNA is replaced by anionic dextran sulfate and released from the polyplexes, the FRET effect disappears, leading to an increase of the bodipy (donor) emission and a decrease of the rhodamine B

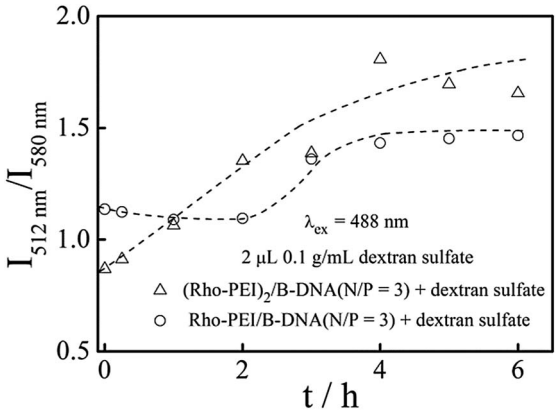

Fig. 6 Time dependence of the replacement of DNA in polyplexes (N/P = 3) in PBS by anionic dextran sulfate (0.1 g mL^{-1}).

(acceptor) emission. In addition, we also used a reducing reagent (TCEP) to cleave the disulfide bond to test its effect on the stability of the polyplexes.

Fig. 7 shows that after treatment with the reducing reagent TCEP, the intensity ratio of the fluorescence emitted at two different wavelengths by Rho-PEI/DNA remains constant, but that of $(Rho\text{-}PEI)_2$/B-DNA gradually decreases and approaches that of Rho-PEI/DNA because the cleavage of the disulfide bond in each $(Rho\text{-}PEI)_2$ chain separates two closely linked rhodamine B molecules and removes the self-quenching so that the fluorescence emitted at 580 nm increases. The combination of the above results demonstrates that $(Rho\text{-}PEI)_2$ is an effective probe for the evaluation of when and where the disulfide bond is cleaved as well as at which point DNA is released inside the cell.

In order to avoid interference by fluorescence generated by uncomplexed free PEI chains in the study of the intracellular trafficking, all the fluorescence labeled PEI/DNA polyplexes were prepared at N/P = 3 with an additional 7-fold unlabeled

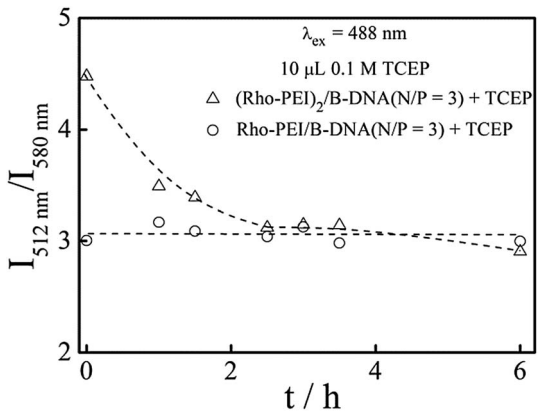

Fig. 7 Time dependence of the fluorescence intensity ratio (I_{512}/I_{580}) of $(Rho\text{-}PEI)_2$/B-DNA and Rho-PEI/DNA polyplexes (N/P = 3) in PBS after treatment with tris(2-carboxyethyl)-phosphine hydrochloride (TCEP, 0.1 M, a reducing reagent to cleave the –S–S– bond in $(Rho\text{-}PEI)_2$).

free lPEI, so that the final N/P ratio remains 10.[21,22] It should be noted that the additional 7-fold of unlabeled lPEI chains do not replace the labeled ones, which combine with DNA in the polyplexes within our experimental time window because the two oppositely charged macromolecular chains interact *via* multi-point electrostatic interactions driven by the entropy gain of counter ions.

Fig. 8a shows that after endocytosis of the lPEI/B-DNA polyplexes (a control, no FRET effect here), the emission intensity, as expected, remains nearly constant. Comparatively, the $(Rho\text{-}PEI)_2$/B-DNA polyplexes initially emit less fluorescent light at 512 nm due to the FRET effect between rhodamine B (the acceptor) and bodipy (the donor). The increase in the fluorescence emitted at 512 nm reflects the de-condensation and a gradual release of B-DNA from the polyplexes. In contrast, Fig. 8b shows that the fluorescence emitted by rhodamine B only slightly increases ~10 to 15% in the first ~5 h, and then gradually increases further. Fig. 8b suggests that the disulfide bonds of $(Rho\text{-}PEI)_2$ inside the polyplexes can be cleaved, *i.e.*, the separation of the two initially closely linked rhodamine B molecules at ~5 h after their endocytosis. Furthermore, we carried out additional confocal laser scanning microscopy (CLSM) studies to support the flow cytometry results.

Fig. 9 shows that the cells transfected by $(Rho\text{-}PEI)_2$/DNA polyplexes have yellow-colored spots in the cytoplasm. Two hours after the addition of the polyplexes, DNA is still condensed, reflected in the FRET signal, with some weak green spots. Gradually, the intensity of the green light increases, but the intensity of the red light remains nearly constant, indicating the disappearance of FRET and the de-condensation/release of B-DNA from the polyplexes. 19 hours later, the green light is visible over a large area of the cytosol although its intensity per unit area is still not high, but at the same time, the red light becomes more visible, which is attributed to the cleavage of the disulfide bonds, *i.e.*, the separation of the two closely linked rhodamine B molecules. For comparison, the intracellular trafficking of both the Rho-PEI/B-DNA and Rho-PEI/DNA polyplexes was also studied by flow cytometry and confocal laser scanning microscopy.

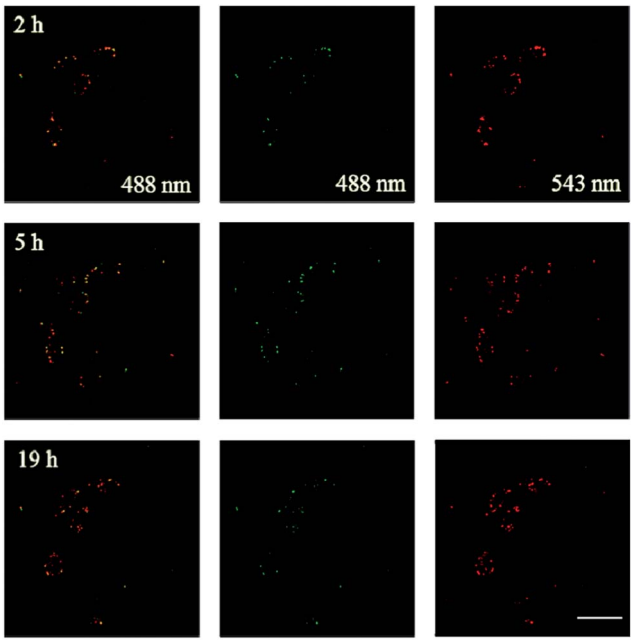

Fig. 9 Confocal laser scanning microscopy imagines of the intracellular trafficking of $(Rho\text{-}PEI)_2$/B-DNA polyplexes, where left: observed at channels 515/30 nm (green) and 605/75 nm (red); middle: observed at channel 515/30 nm (green); and right: observed at channel 605/75 nm (red) (bar = 50 μm).

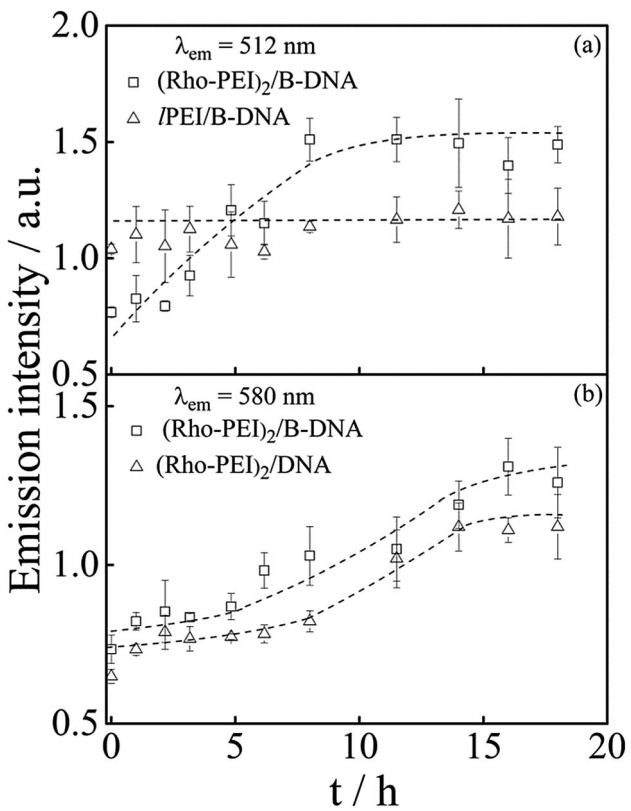

Fig. 8 Time dependence of the fluorescence emission intensity of $(Rho\text{-}PEI)_2$/B-DNA, $(Rho\text{-}PEI)_2$/DNA and lPEI/B-DNA polyplexes measured by flow cytometry, where $\lambda_{excitation}$ = 488 nm.

Fig. 10 shows that during transfection, the emission intensity of the Rho-PEI/B-DNA polyplexes at 512 nm continuously increases, signaling a diminishing of the FRET effect and the de-condensation/release of DNA from the polyplexes. In contrast, the Rho-PEI/B-DNA and Rho-PEI/DNA polyplexes emit a similar intensity at 580 nm. Since there is no disulfide bond in Rho-PEI, there is no –S–S– cleavage or self-quenching. The flow cytometry results are consistent with the confocal microscopy ones, as shown in Fig. 11. Namely, 2 hours after the addition of the polyplexes, the green light (bodipy) is weak due to the FRET effect. As the gene transfection proceeds, the green light intensity gradually increases, reflecting the gradual de-condensation/release of DNA from the Rho-PEI/B-DNA polyplexes. It is worth-noting that after 19 hours, the red light intensity remains nearly constant and observable over a large area of the cytosol, indicating that some polyplexes have

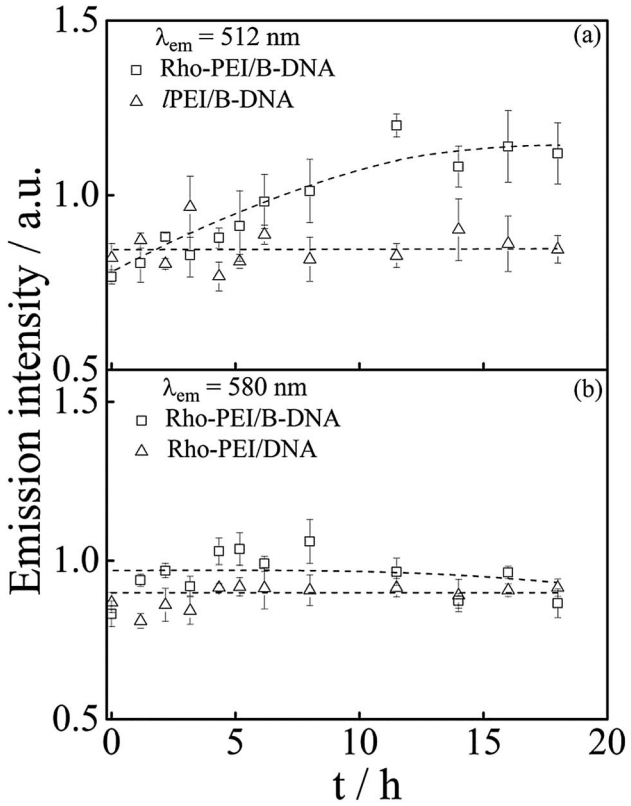

Fig. 10 Time dependence of the intracellular trafficking of Rho-PEI/B-DNA, Rho-PEI/DNA and lPEI/B-DNA polyplexes measured by flow cytometry, where $\lambda_{excitation} = 488$ nm.

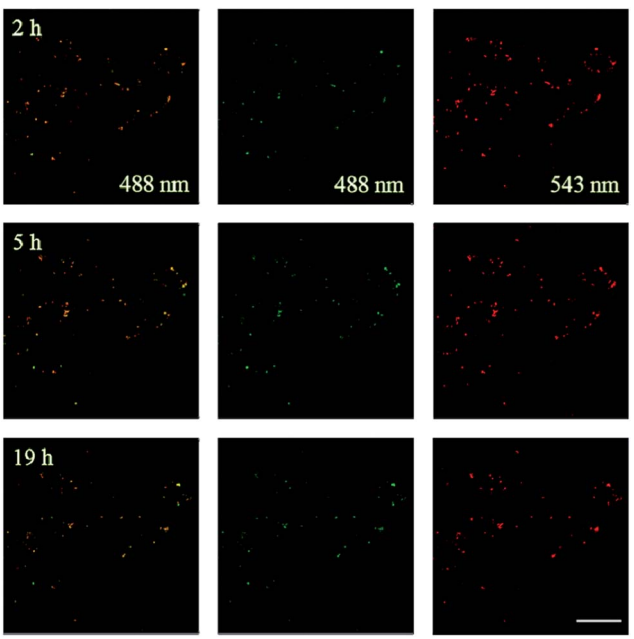

Fig. 11 Confocal laser scanning microscopy imagines of the intracellular trafficking of Rho-PEI/B-DNA polyplexes, where left: observed at channels 515/30 nm (green) and 605/75 nm (red); middle: observed at channel 515/30 nm (green); and right: observed at channel 605/75 nm (red) (bar = 50 μm).

already escaped from the endosomes and entered into the cytosol.

The flow cytometry and CLSM results reveal that (1) the release of DNA condensed by linear PEI inside the polyplexes occurs continuously after intracellular uptake; (2) there is no visible fluorescence inside the nucleus even after 19 h, at which the gene transcription has started, indicating that the number of polyplexes entering the nucleus must be very low; and (3) the cleavage of the disulfide bonds occurs at about 5 h after the removal of the transfection reagent, notably, there is no strong correlation between the cleavage of the disulfide linkage and the release of DNA from the polyplexes. In order to locate where the disulfide bonds are cleaved inside the cell, we labeled early endosomes with Celllight early endosomes-GFP and lysosomes with Lysosensor™ Green.

Fig. 12 and S11† show that initially most of polyplexes were attached to the cellular membranes and endocytosis occurs gradually. Note that the fluorescence signals of rhodamine and GFP are separated in the cytoplasm; as there are few observable colocalized yellow spots, indicating the escape of some polyplexes before they reach the early endosomes.

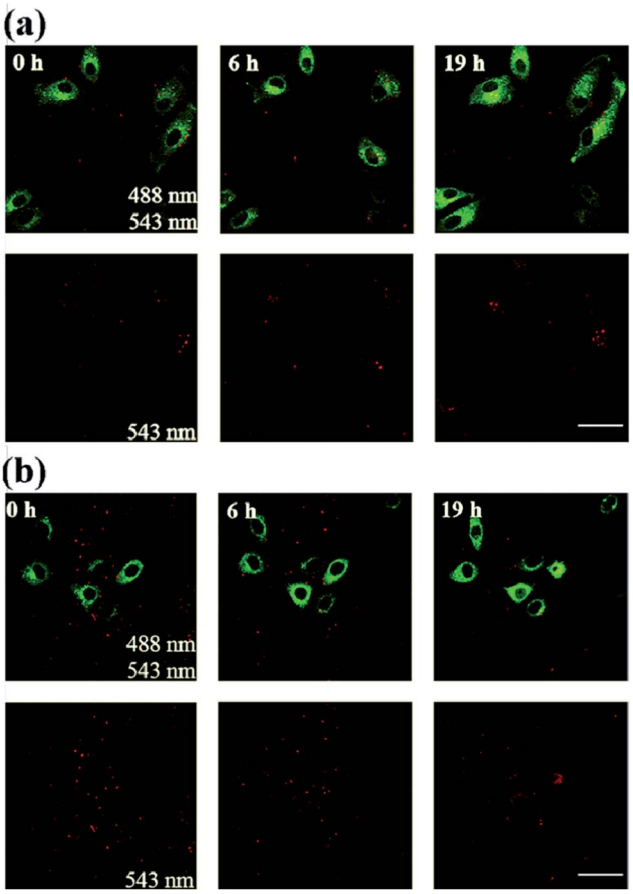

Fig. 12 Colocalization of (a) $(Rho-PEI)_2$/DNA and (b) Rho-PEI/DNA polyplexes with early endosomes labeled by Celllight early endosomes-GFP. In each case, the upper panel: observed at channel 515/30 nm (green) and channel 605/75 nm (red); and lower panel: observed at channel 605/75 nm (red) (bar = 50 μm).

Therefore, it seems that the intracellular trafficking of some polyplexes does not follow the normal early endosome–late endosome–endolysosome pathway. In addition, Fig. 13a and S12a† show that the colocalization of $(Rho\text{-}PEI)_2$/DNA polyplexes and lysosomes appears after 3 h, and subsequently both red and yellow spots are observable inside the cells, further indicating that some of the polyplexes have escaped from the endosomes, reflecting the red spots in the cytosol; and the rest are accumulated in the lysosomes, reflecting the increased yellow light intensity.

Fig. 13a also shows the increase in intensity of the red light in the lysosomes, attributed to the cleavage of the disulfide bond that links the two rhodamine B molecules together, *i.e.*, self-dequenching. A similar colocalization between the polyplexes and lysosomes is also observed for Rho-PEI/DNA polyplexes, as shown in Fig. 13b and S12b.† As expected, the intensity of the red light in the lysosome remains the same even after 19 h because there is no disulfide bond to be cleaved here. The above results reveal that the disulfide bonds in PEI chains are cleaved in the lysosomes, although some polyplexes have escaped from the endosomes before cleavage. Scheme 2 summarizes the intracellular trafficking of degradable PEI/DNA polyplexes.

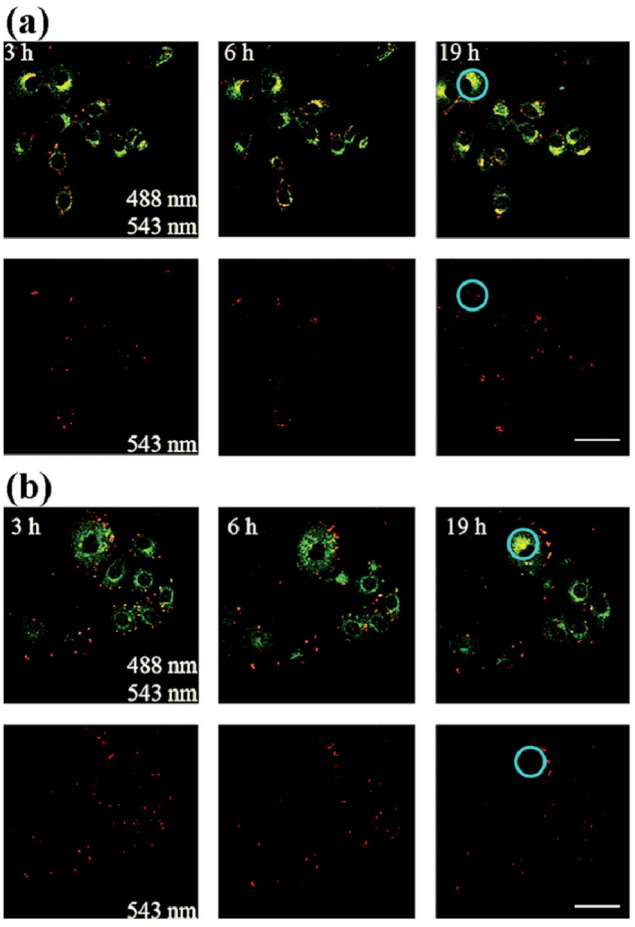

Fig. 13 Colocalization of (a) $(Rho\text{-}PEI)_2$/DNA and (b) Rho-PEI/DNA polyplexes with lysosomes labeled by Lysosensor™ Green. In each case, the upper panel: observed at channel 515/30 nm (green) and channel 605/75 nm (red); and lower panel: observed at channel 605/75 nm (red) (bar = 50 μm).

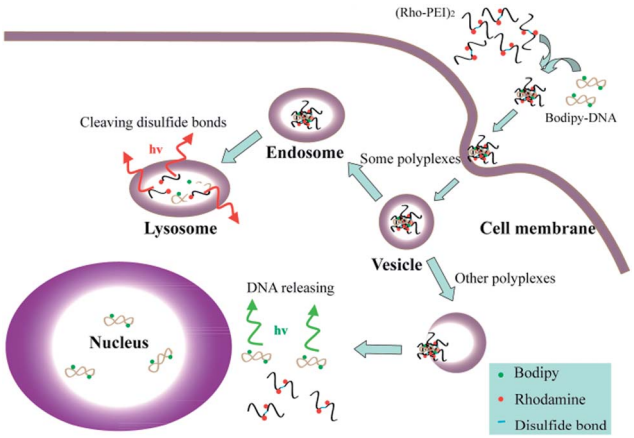

Scheme 2 Schematic of when and where disulfide bonds inside PEI/DNA polyplexes are cleaved and polyplexes escape from endosome during intracellular trafficking.

4. Conclusions

Coupling two short linear PEI chains together with rhodamine B and a disulfide linker leads to an effective fluorescent probe, which can be applied to trace the intracellular trafficking of ingested polyplexes. This probe has higher transfection efficiency and lower cytotoxicity compared to commercial PEIs. Labeling plasmid DNA with bodipy, a FRET donor of rhodamine B, further enables us to analyze FRET and self-dequenching of the polyplexes inside the HepG2 cell. We found that soon after endocytosis, DNA is continuously de-condensed/released from the polyplexes prior to the cleavage of the disulfide bonds so that there is little correlation between the cleavage of the disulfide linkage and the release of DNA from the polyplexes. Some of the PEI/DNA polyplexes escape from the endosomes rapidly, and the disulfide bonds of entrapped polyplexes are cleaved inside the lysosomes, which occurs at ~5 h after endocytosis.

Acknowledgements

The financial support of the National Natural Scientific Foundation Projects (20934005 and 51173177), the Ministry of Science and Technology Key Project (2012CB933802), and the Hong Kong SAR Earmarked Projects (CUHK4036/11P, 2130281; 2060431 and CUHK7/CRF/12G) is gratefully acknowledged.

Notes and references

1 D. W. Pack, A. S. Hoffman, S. Pun and P. S. Stayton, *Nat. Rev. Drug Discovery*, 2005, **4**, 581–593.
2 A. Rolland, *Adv. Drug Delivery Rev.*, 2005, **57**, 669–673.
3 I. M. Verma and N. Somia, *Nature*, 1997, **389**, 239–242.

4 P. L. Felgner, T. R. Gadek, M. Holm, R. Roman, H. W. Chan, M. Wenz, J. P. Northrop, G. M. Ringold and M. Danielsen, *Proc. Natl. Acad. Sci. U. S. A.*, 1987, **84**, 7413–7417.
5 Y. Z. Ma, S. Hou, B. Ji, Y. Yao and X. Z. Feng, *Macromol. Biosci.*, 2010, **10**, 202–210.
6 Y. Yao, D. F. Feng, Y. P. Wu, Q. J. Ye, L. Liu, X. X. Li, S. Hou, Y. L. Yang, C. Wang, L. Li and X. Z. Feng, *J. Mater. Chem.*, 2011, **21**, 4538–4545.
7 O. Boussif, F. Lezoualch, M. A. Zanta, M. D. Mergny, D. Scherman, B. Demeneix and J. P. Behr, *Proc. Natl. Acad. Sci. U. S. A.*, 1995, **92**, 7297–7301.
8 D. Fischer, T. Bieber, Y. X. Li, H. P. Elsasser and T. Kissel, *Pharm. Res.*, 1999, **16**, 1273–1279.
9 A. Akinc and R. Langer, *Biotechnol. Bioeng.*, 2002, **78**, 503–508.
10 A. Akinc, M. Thomas, A. M. Klibanov and R. Langer, *J. Gene Med.*, 2005, **7**, 657–663.
11 M. Breunig, U. Lungwitz, R. Liebl and A. Goepferich, *Eur. J. Pharm. Biopharm.*, 2006, **63**, 156–165.
12 Y. Matsumoto, K. Itaka, T. Yamasoba and K. Kataoka, *J. Gene Med.*, 2009, **11**, 615–623.
13 G. Grandinetti and T. M. Reineke, *Mol. Pharm.*, 2012, **9**, 2256–2267.
14 C. Pichon, L. Billiet and P. Midoux, *Curr. Opin. Biotechnol.*, 2010, **21**, 640–645.
15 S. N. Xiang, H. J. Tong, Q. Shi, J. C. Fernandes, T. Jin, K. R. Dai and X. L. Zhang, *J. Controlled Release*, 2012, **158**, 371–378.
16 A. Baker, M. Saltik, H. Lehrmann, I. Killisch, V. Mautner, G. Lamm, G. Christofori and M. Cotten, *Gene Ther.*, 1997, **4**, 773–782.
17 W. T. Godbey, K. K. Wu and A. G. Mikos, *J. Controlled Release*, 1999, **60**, 149–160.
18 W. T. Godbey, K. K. Wu and A. G. Mikos, *Proc. Natl. Acad. Sci. U. S. A.*, 1999, **96**, 5177–5181.
19 K. Itaka, A. Harada, Y. Yamasaki, K. Nakamura, H. Kawaguchi and K. Kataoka, *J. Gene Med.*, 2004, **6**, 76–84.
20 Z. J. Dai and C. Wu, *Macromolecules*, 2012, **45**, 4346–4353.
21 Y. A. Yue, F. Jin, R. Deng, J. G. Cai, Y. C. Chen, M. C. M. Lin, H. F. Kung and C. Wu, *J. Controlled Release*, 2011, **155**, 67–76.
22 Y. A. Yue, F. Jin, R. Deng, J. G. Cai, Z. J. Dai, M. C. M. Lin, H. F. Kung, M. A. Mattebjerg, T. L. Andresen and C. Wu, *J. Controlled Release*, 2011, **152**, 143–151.
23 S. Bauhuber, C. Hozsa, M. Breunig and A. Gopferich, *Adv. Mater.*, 2009, **21**, 3286–3306.
24 M. Breunig, U. Lungwitz, R. Liebl and A. Goepferich, *Proc. Natl. Acad. Sci. U. S. A.*, 2007, **104**, 14454–14459.
25 R. Deng, Y. Yue, F. Jin, Y. C. Chen, H. F. Kung, M. C. M. Lin and C. Wu, *J. Controlled Release*, 2009, **140**, 40–46.
26 H. Koo, G. W. Jin, H. Kang, Y. Lee, K. Nam, C. Z. Bai and J. S. Park, *Biomaterials*, 2010, **31**, 988–997.
27 N. Zhao, S. Roesler and T. Kissel, *Int. J. Pharm.*, 2011, **411**, 197–205.
28 Y. Lee, H. Mo, H. Koo, J. Y. Park, M. Y. Cho, G. W. Jin and J. S. Park, *Bioconjugate Chem.*, 2007, **18**, 13–18.
29 J. Yang, H. Chen, I. R. Vlahov, J. X. Cheng and P. S. Low, *Proc. Natl. Acad. Sci. U. S. A.*, 2006, **103**, 13872–13877.
30 C. D. Austin, X. H. Wen, L. Gazzard, C. Nelson, R. H. Scheller and S. J. Scales, *Proc. Natl. Acad. Sci. U. S. A.*, 2005, **102**, 17987–17992.
31 J. R. Lakowicz, J. Malicka, S. D'Auria and I. Gryczynski, *Anal. Biochem.*, 2003, **320**, 13–20.
32 J. R. Lakowicz, J. Malicka, S. D'Auria and I. Gryczynski, *Biophys. J.*, 2003, **84**, 291a.
33 D. Setiawan, A. Kazaryan, M. A. Martoprawiro and M. Filatov, *Phys. Chem. Chem. Phys.*, 2010, **12**, 11238–11244.